

Synthesis and Structural Determination of 2D Ladder-Like Mononuclear Nine-Coordinate (EnH_2) $[\text{Nd}^{\text{III}}(\text{Egta})\text{H}_2\text{O}]_2 \cdot 6\text{H}_2\text{O}$ and Ten-Coordinate (EnH_2) $_{1.5}[\text{Nd}^{\text{III}}(\text{Ttha})] \cdot 5\text{H}_2\text{O}$ ¹

F. Y. Tian, G. H. Liu, B. Li, Y. T. Song, and J. Wang*

Department of Chemistry, Liaoning University, Shenyang, 110036 P.R. China

*e-mail: wangjuncomplex890@126.com

Received February 27, 2016

Abstract—Two novel lanthanide complexes, $(\text{EnH}_2)[\text{Nd}^{\text{III}}(\text{Egta})\text{H}_2\text{O}]_2 \cdot 6\text{H}_2\text{O}$ (**I**) and $(\text{EnH}_2)_{1.5}[\text{Nd}^{\text{III}}(\text{Ttha})] \cdot 5\text{H}_2\text{O}$ (**II**), where En = ethylenediamine, H_4Egta = ethyleneglycol-bis-(2-aminoethylether)- N,N,N',N' -tetraacetic acid and H_6Ttha = triethylenetetramine- N,N,N',N'',N''',N'''' -hexaacetic acid, have been successfully synthesized through direct heating reflux and their molecular and crystal structures were determined by FT-IR spectroscopy, thermal analysis and single crystal X-ray diffraction (CIF files CCDC nos. 1436598 (**I**) and 1433221 (**II**)). X-ray diffraction reveals that **I** has a nine-coordinate mononuclear structure with pseudo-monocapped square antiprismatic conformation. Complex **I** crystallizes in a monoclinic system with $P2_1/c$ space group; $a = 13.0919(12)$, $b = 12.6840(11)$, $c = 16.9751(14)$ Å, $\beta = 122.069(3)^\circ$ and $V = 2388.7(4)$ Å³. Complex **II** takes ten-coordinated structure with a distorted bicapped square antiprismatic prism belong to triclinic crystal system with $P\bar{1}$ space group; $a = 9.9376(10)$, $b = 12.2178(12)$, $c = 15.2671(16)$, $\beta = 100.2480(10)^\circ$ and $V = 1609.5(3)$ Å³. Each EnH_2^{2+} cation in **I** connects four adjacent $[\text{Nd}^{\text{III}}(\text{Egta})\text{H}_2\text{O}]^-$ anions through hydrogen bonds. In **II** crystal cell, there are two types of EnH_2^{2+} cations, which form hydrogen bonds with the neighboring $[\text{Nd}^{\text{III}}(\text{Ttha})]^{3-}$ anions, leading to the formation of a 2D ladder-like layer structure. The results showed that the change of ligands can lead to change of the structure of the complexes, coordination numbers and coordination geometries. Thus, it can be concluded that the shape of ligands play a crucial role on the coordinate structure of complexes, coordination numbers and coordination geometries.

Kyewords: synthesis, structural determination, nine-coordinate, ten-coordinate, Nd(III) complex

DOI: 10.1134/S1070328417050074

INTRODUCTION

Within recent years, due to the unique physical and chemical properties of lanthanide ions, lanthanide complexes are of great importance in industrial, chemical, medical, and sensor applications [1, 2]. In particular, rare earth complexes are applied as magnetic resonance imaging (MRI) contrast agent [3, 4], shift reagents for nuclear magnetic resonance (NMR) spectroscopy [5], luminescent chemosensors and probes for medical diagnostics [6–9]. For instance, Pr(III) in solids exhibits prominent optical features [10]. Sm^{III}-EDTMP (EDTMP = ethylenediamine- N,N,N',N' -tetramethyleneephosphonate) has been reported to have high-efficiency and long-lasting treatment of nasopharyngeal, breast carcinoma, lung cancer, and prostate carcinoma [11, 12]. Tb^{III} and Eu^{III} complexes with aminopolycarboxylic acid

ligands have unusual spectroscopic characteristics, so they have been used as probes in fluoroimmunoassay [13] and as sensors for certain bioactive ions [14]. Moreover, Nd(III) complexes have good anti-inflammation activity [15, 16]. The electroluminescence application of Nd(III) complexes were widely studied and Nd(III) complex-based OLEDs have been reported several times [17, 18]. Of course, these applications all are based on the understanding of the characters of the rare-earth or radioactive rare-earth metal complexes in detail. For these reasons given above, it is necessary to determine and study the crystal and molecular structures of rare-earth metal complexes with aminopolycarboxylic acids.

In general, structures and coordination numbers of most rare-earth metal complexes depend on the ionic radii, electronic configuration of central metal ions and the counter ion species as well as the shape of ligands. The rare-earth metal ions can form the

¹ The article is published in the original.

eight-, nine- and ten-coordinate complexes with aminopolycarboxylic acid ligands since they have different ionic radii and electronic configurations. Taking rare earth metal complexes with ethyleneglycol-bis-(2-aminoethylether)-*N,N,N',N'*-tetraacetic acid (H_4Egta) ligand and ethylenediamine (En) as counter ion for example, these complexes always form nine-coordinate complexes, except for Lu^{3+} ion with the smallest ionic radius among all rare earth metal ions, which forms eight-coordinate complex. So, we wonder that rare earth metal complexes with H_4Egta ligand and ethylenediamine counter ion only could form eight- and nine-coordinate complexes. Hence, we chose the Nd^{3+} ion with larger ionic radius as central metal ion and predict that it could form the nine-coordinate complexes with H_4Egta ligand and ethylenediamine counter ion. Meanwhile, taking rare earth metal complexes with triethylenetetraaminehexaacetic acid (H_6Ttha) ligand and ethylenediamine as counter ion for example, we found that $(EnH_2)_{1.5}[Sm^{III}(Ttha)] \cdot 4.5H_2O$ [19], $(EnH_2)_3[Eu^{III}(Ttha)]_2 \cdot 11H_2O$ [20], $(EnH_2)_3[Gd^{III}(Ttha)]_2 \cdot 11H_2O$ [21], $(EnH_2)_3[Tb^{III}(Ttha)]_2 \cdot 11H_2O$ [22], $(EnH_2)_3[Dy^{III}(Ttha)]_2 \cdot 9H_2O$ [23], $(EnH_2)_{1.5}[Ho^{III}(Ttha)] \cdot 4.5H_2O$ [24] and $(EnH_2)_{1.5}[Er^{III}(Ttha)] \cdot 3H_2O$ [25] all form nine coordinate complexes. However, for the Nd^{3+} ion with the relatively large ionic radii of 0.1123 nm and electronic configurations f^3 , we speculate that it should form nine- or ten-coordinate structure with H_6Ttha . Through comparison the two $Nd(III)$ complexes with the same counter ion and different ligand, we also want to know how ligand species generate effects upon coordination number, coordination structure, space group, molecular structure and crystal structure.

In order to validate this supposition and extend our work, fortunately, two novel rare earth metal complex with H_4Egta and H_6Ttha ligand, namely, $(EnH_2)[Nd^{III}(Egta)H_2O]_2 \cdot 6H_2O$ (**I**) and $(EnH_2)_{1.5}[Nd^{III}(Ttha)] \cdot 5H_2O$ (**II**), were successfully synthesized. As expected, **I** adopts nine-coordinate mononuclear structure with pseudo-monocapped square antiprismatic configuration, and **II** takes ten-coordinated structure with a distorted bicapped square antiprismaticprism. However, due to the different structures of aminopolycarboxylic acid ligands, **I** and **II** have also some differences in coordinate structure, molecular structure and space group and so on. In addition, this study supports the idea that the structures of the rare-earth metal complexes with aminopolycarboxylic acid are mainly determined by the radii of the central metal ions as mentioned above, ligand structure and counter ion. Nevertheless, **I** and **II** all adopt 2D ladder-like network through hydrogen bonds formed between ethylenediamine and

$[Nd^{III}(Egta)H_2O]^-$ and $[Nd^{III}(Ttha)]^{3-}$ complex anions. Compared the two $Nd(III)$ complexes with fixed rare earth metal and counter ion, we draw a conclusion that their coordinate structures and molecular structures sometimes are related to the shape of ligands. Hence, the different structures of aminopolycarboxylic acid ligands have vital effect on the coordinate structure, molecular structures and crystal structure.

EXPERIMENTAL

Materials and methods. Nd_2O_3 powder (99.999%, Yuelong Rare Earth Co., Ltd., China), and ligand of H_4Egta (A.R., Beijing SHLHT Science and Trade Co., Ltd., China) and H_6Ttha (A.R., Beijing SHLHT Science and Trade Co., Ltd., China) were used to synthesize the title aminopolycarboxylic acid complexes. In addition, En aqueous solution was slowly added to above solution in order to adjust the pH to 6.0. The structure of complexes was detected by X-ray equipment (XT-V130, Beijing Xinzhuo, Company, China).

Synthesis of I. H_4Egta (1.9017 g, 5.0 mmol) was added to 100 mL warm water and Nd_2O_3 powder was slowly added to above solution. After the mixture, had been stirred and refluxed for 18.0 h, the solution became transparent. And then the pH value was also adjusted to 6.0 by dilute ethylenediamine En aqueous solution. Finally, the solution was concentrated to 25 mL. A light brown crystal appeared after three weeks at room temperature. The yield was 2.11 g (81.92%).

Synthesis of II. H_6Ttha (2.47 g, 5.0 mmol) was added to 100 mL warm water and Nd_2O_3 powder (0.8412 g, 2.5 mmol) was slowly added to above solution. After the mixture, had been stirred and refluxed for 18.0 h, the solution became transparent. And then the pH value was also adjusted to 6.0 by dilute En aqueous solution. Finally, the solution was concentrated to 25 mL. A light brown crystal appeared after two weeks at room temperature. The yield was 2.64 g (83.46%).

X-ray structure determination. X-ray intensity data of **I** and **II** samples were collected on a Bruker SMART CCD type X-ray diffractometer system with graphite-monochromatized MoK_{α} radiation ($\lambda = 0.71073 \text{ \AA}$) using $\varphi-\omega$ scan technique in the range of $1.72^\circ \leq \theta \leq 26.00^\circ$. Their structures were solved by direct methods. All non-hydrogen atoms were refined anisotropically by full-matrix least-squares methods on F^2 . All the calculations were performed by the SHELXTL-97 program on PDP11/44 and Pentium MMX/166 computers. The crystal data and structure refinement for two complexes were listed in Table 1. And the selected bond distances and bond angles of two complexes were listed in Table 2.

Table 1. Crystallographic data and structure refinements for **I** and **II**

Parameter	Value	
	I	II
Empirical formula	C ₃₀ H ₆ N ₃ Nd ₂ O ₂₈	C ₂₁ H ₄₉ N ₇ NdO ₁₇
Formula weight	1247.37	815.91
Temperature, K	298(2)	293(2)
Wavelength, Å	0.71073	0.71073
Crystal system	Monoclinic	Triclinic
Space group	<i>P</i> 2 ₁ /c	<i>P</i> 1̄
Unit cell dimensions:		
<i>a</i> , Å	13.0919(12)	9.9376(10)
<i>b</i> , Å	12.6840(11)	12.2178(12)
<i>c</i> , Å	16.9751(14)	15.2671(16)
α, deg		111.277(2)
β, deg	122.069(3)	100.2480(10)
γ, deg		103.315(2)
Volume, Å ³	2388.7(4)	1609.5(3)
<i>Z</i>	2	2
ρ _{calcd} , g/cm ³	1.734	1.684
Absorption coefficient, mm ⁻¹	2.245	1.698
<i>F</i> (000)	1264	840
Crystal size, mm	0.28 × 0.13 × 0.08	0.37 × 0.18 × 0.13
θ range for data collection, deg	2.28–25.01	2.74–25.02
Limiting indices	−8 ≤ <i>h</i> ≤ 15, −15 ≤ <i>k</i> ≤ 15, −20 ≤ <i>l</i> ≤ 19	−11 ≤ <i>h</i> ≤ 11, −14 ≤ <i>k</i> ≤ 14, −18 ≤ <i>l</i> ≤ 18
Reflections collected	11785	10535
Independent reflections (<i>R</i> _{int})	4219 (0.0339)	5688 (0.0657)
Completeness to θ _{max} , %	100.0	99.9
Max and min transmission	0.5408 and 0.5721	0.7661 and 0.5787
Goodness-of-fit on <i>F</i> ²	1.086	1.039
Final <i>R</i> indices (<i>I</i> > 2σ(<i>I</i>))	<i>R</i> ₁ = 0.0292, <i>wR</i> ₂ = 0.0612	<i>R</i> ₁ = 0.0575, <i>wR</i> ₂ = 0.1134
<i>R</i> indices (all data)	<i>R</i> ₁ = 0.0466, <i>wR</i> ₂ = 0.0693	<i>R</i> ₁ = 0.0863, <i>wR</i> ₂ = 0.1344
Largest difference peak and hole, <i>e</i> Å ⁻³	1.165 and −0.636	1.382 and −0.993
Absorption correction	Empirical	
Refinement method	Full-matrix least-squares on <i>F</i> ²	

Supplementary material has been deposited with the Cambridge Crystallographic Data Centre (CCDC nos. 1436598 (**I**) and 1433221 (**II**); deposit@ccdc.cam.ac.uk or <http://www.ccdc.cam.ac.uk>).

RESULTS AND DISCUSSION

FT-IR spectra between H₄Egta and **I** reveals that the v(C—N) of **I** appears at 1068 cm⁻¹, which displays red-shifts by 67 cm⁻¹ compared with that (1135 cm⁻¹)

of H₄Egta. This suggests that the amine nitrogen atoms of the H₄Egta ligand are coordinated to the Nd³⁺ ion. The spectrum of free H₄Egta ligand shows strong absorption band around 1736 cm⁻¹ originating from stretching vibrations of carbonyl group v(C=O), which disappears completely in the FT-IR spectrum of complex **I**. Furthermore, **I** gives the characteristic absorption peaks of carboxyl groups at 1602 cm⁻¹ for the asymmetric stretching vibration, revealing a red-

Table 2. Selected bond distances (Å) and angles (deg) of **I** and **II**

Bond	<i>d</i> , Å	Bond	<i>d</i> , Å	Bond	<i>d</i> , Å
I					
Nd(1)–O(1)	2.576(3)	Nd(1)–O(5)	2.427(3)	Nd(1)–O(11)	2.535(3)
Nd(1)–O(2)	2.532(3)	Nd(1)–O(7)	2.407(3)	Nd(1)–N(1)	2.679(3)
Nd(1)–O(3)	2.430(3)	Nd(1)–O(9)	2.426(3)	Nd(1)–N(2)	2.695(3)
II					
Nd(1)–O(1)	2.467(4)	Nd(1)–O(9)	2.501(5)	Nd(1)–N(3)	2.727(6)
Nd(1)–O(3)	2.461(6)	Nd(1)–O(11)	2.586(6)	Nd(1)–N(4)	2.789(7)
Nd(1)–O(5)	2.455(4)	Nd(1)–N(1)	2.761(6)		
Nd(1)–O(7)	2.505(5)	Nd(1)–N(2)	2.719(6)		
Angle	ω , deg	Angle	ω , deg	Angle	ω , deg
I					
O(1)Nd(1)O(2)	66.54(10)	O(2)Nd(1)O(11)	65.57(9)	O(5)Nd(1)N(1)	63.69(10)
O(1)Nd(1)O(3)	122.79(9)	O(2)Nd(1)N(1)	131.22(10)	O(5)Nd(1)N(2)	148.04(11)
O(1)Nd(1)O(5)	91.55(10)	O(2)Nd(1)N(2)	66.96(10)	O(7)Nd(1)O(9)	126.78(9)
O(1)Nd(1)O(7)	157.12(10)	O(3)Nd(1)O(5)	90.65(10)	O(7)Nd(1)O(11)	75.53(10)
O(1)Nd(1)O(9)	67.87(9)	O(3)Nd(1)O(7)	79.92(10)	O(7)Nd(1)N(1)	129.35(10)
O(1)Nd(1)O(11)	82.05(10)	O(3)Nd(1)O(9)	140.23(10)	O(7)Nd(1)N(2)	64.82(10)
O(1)Nd(1)N(1)	67.39(10)	O(3)Nd(1)O(11)	149.51(10)	O(9)Nd(1)O(11)	135.02(10)
O(1)Nd(1)N(2)	120.32(10)	O(3)Nd(1)N(1)	62.91(10)	O(9)Nd(1)N(1)	76.84(10)
O(2)Nd(1)O(3)	137.30(10)	O(3)Nd(1)N(2)	74.70(10)	O(9)Nd(1)N(2)	63.65(10)
O(2)Nd(1)O(5)	132.01(9)	O(5)Nd(1)O(7)	84.96(10)	O(11)Nd(1)N(1)	122.05(10)
O(2)Nd(1)O(7)	99.40(10)	O(5)Nd(1)O(9)	140.23(10)	O(11)Nd(1)N(2)	109.80(10)
O(2)Nd(1)O(9)	71.91(10)	O(5)Nd(1)O(11)	69.58(10)	N(1)Nd(1)N(2)	128.03(10)
II					
O(1)Nd(1)O(3)	82.72(18)	O(3)Nd(1)N(3)	132.18(18)	O(9)Nd(1)O(11)	93.33(18)
O(1)Nd(1)O(5)	146.14(17)	O(3)Nd(1)N(4)	124.37(17)	O(9)Nd(1)N(1)	119.09(18)
O(1)Nd(1)O(7)	87.13(15)	O(5)Nd(1)O(7)	125.54(15)	O(9)Nd(1)N(2)	128.08(18)
O(1)Nd(1)O(9)	78.72(15)	O(5)Nd(1)O(9)	72.55(16)	O(9)Nd(1)N(3)	120.61(17)
O(1)Nd(1)O(11)	68.49(18)	O(5)Nd(1)O(11)	129.81(17)	O(9)Nd(1)N(4)	60.06(19)
O(1)Nd(1)N(1)	60.71(17)	O(5)Nd(1)N(1)	119.76(18)	O(11)Nd(1)N(1)	109.31(17)
O(1)Nd(1)N(2)	126.91(18)	O(5)Nd(1)N(2)	63.79(16)	O(11)Nd(1)N(2)	136.10(18)
O(1)Nd(1)N(3)	142.97(18)	O(5)Nd(1)N(3)	69.52(17)	O(11)Nd(1)N(3)	78.48(18)
O(1)Nd(1)N(4)	107.87(17)	O(5)Nd(1)N(4)	72.70(17)	O(11)Nd(1)N(4)	59.08(16)
O(3)Nd(1)O(5)	70.88(17)	O(7)Nd(1)O(9)	157.12(17)	N(1)Nd(1)N(2)	66.28(17)
O(3)Nd(1)O(7)	126.57(18)	O(7)Nd(1)O(11)	64.58(17)	N(1)Nd(1)N(3)	119.05(18)
O(3)Nd(1)O(9)	69.67(18)	O(7)Nd(1)N(1)	67.05(18)	N(1)Nd(1)N(4)	107.87(17)
O(3)Nd(1)O(11)	149.19(17)	O(7)Nd(1)N(2)	74.79(17)	N(2)Nd(1)N(3)	68.6(2)
O(3)Nd(1)N(1)	62.29(17)	O(7)Nd(1)N(3)	63.17(16)	N(2)Nd(1)N(4)	125.16(17)
O(3)Nd(1)N(2)	70.53(19)	O(7)Nd(1)N(4)	108.70(18)	N(3)Nd(1)N(4)	65.94(19)

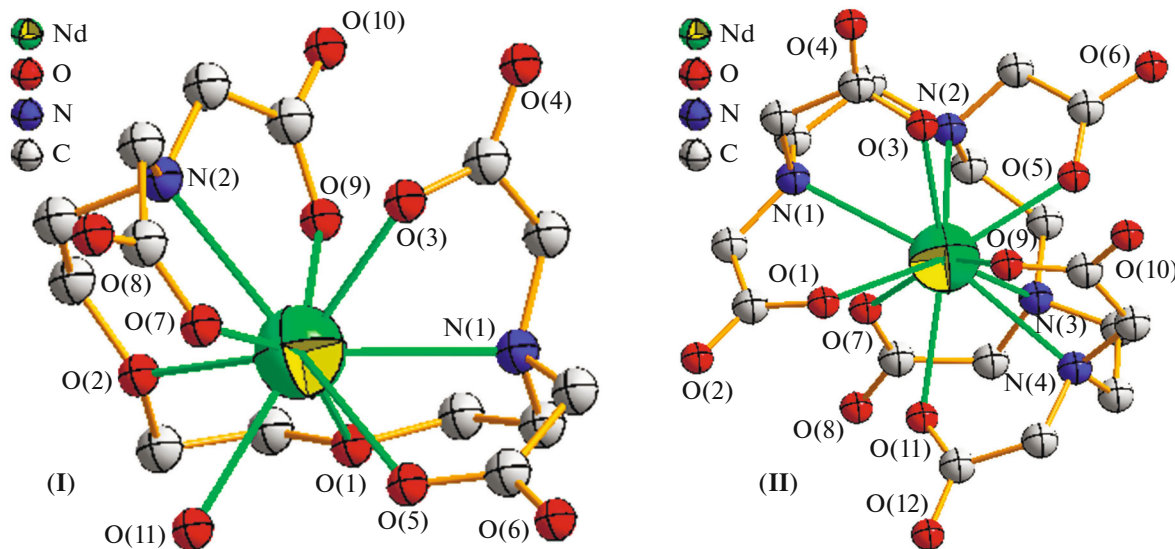


Fig. 1. Molecular structures of **I** and **II**.

shift (35 cm^{-1}) compared with 1637 cm^{-1} of H_4Egta . The $\nu_s(\text{COO})$ band of **I** appears at 1400 cm^{-1} , showing a blue-shift (13 cm^{-1}) compared with that (1397 cm^{-1}) of H_4Egta . These changes in the peak position confirm that the oxygen atoms from the carboxyl groups are also coordinated to the Nd^{3+} ion. Besides, there is a broad absorption band near 3382 cm^{-1} for **I**. It could be reasonably attributed to the stretching vibration absorption peak of O–H bond.

Similarly, the $\nu(\text{C–N})$ of **II** appears at 1096 cm^{-1} , which displays a red-shift (197 cm^{-1}) compared with that (899 cm^{-1}) of H_6Ttha , indicating that the amine nitrogen atoms of H_6Ttha ligand are coordinated to the Nd^{3+} ion. The $\nu_{as}(\text{COOH})$ band of H_6Ttha at 1736 cm^{-1} disappears in the FT-IR spectrum of the complex **II**. In addition, **II** gives the characteristic absorption peaks of carboxyl groups at 1591 cm^{-1} for the asymmetric stretching vibration and at 1402 cm^{-1} for symmetric stretching vibration, revealing a blue-shift (121 cm^{-1}) compared with that (1470 cm^{-1}) of H_6Ttha and a red-shift (12 cm^{-1}) compared with that (1414 cm^{-1}) of H_6Ttha . These results clearly show that oxygen in carboxylates participate in coordination to $\text{Nd}(\text{III})$. Also, a strong and wide absorption band around 3415 cm^{-1} in **II** could be reasonably assigned to O–H stretch.

The TG curve of **I** roughly shows a three-stage decomposition pattern. The first stage weight loss is about 7.72% from room temperature to 101°C , which corresponds to release of six water molecules; weight loss of 2.89% from 101 to 148°C corresponds to the releases of two coordinated water molecules. From 148 to 246°C , there is small weight loss, which means that the crystal structure is stable until 246°C . The second

weight loss of 10.12% from 257 to 346°C should correspond to the expulsion of ethylenediamine. The last stage weight loss is attributed to the decomposition of the organic ligand starting from 346 to 800°C , the weight loss ratio is about 35.69%. The final residue is mainly Nd_2O_3 , the overall weight loss ratio is about 56.42% according to the mass calculation.

The thermal decomposition process of **II** complex displays similar thermal behavior with **I**. The first thermal decomposition happens from 25 to 258°C . In this step the weight loss ratio is about 9.45%, which corresponds to the releasing five lattice water molecules. The second weight loss of 20.54% from 258 to 347°C corresponds to the expulsion ethylenediamine. Then, the sample decomposes gradually and the decomposition is completed at 800°C . The corresponding weight loss is about 34.79%, and the corresponding final remainder is mainly Nd_2O_3 . The total weight loss ratio is about 64.78% according to the mass calculation.

As seen from Fig. 1a, that $\text{Nd}(\text{III})$ forms (1 : 1) nine-coordinate complex with the Egta ligand, which is similar to that of $(\text{EnH}_2)[\text{Sm}^{\text{III}}(\text{Egta})(\text{H}_2\text{O})]_2 \cdot 6\text{H}_2\text{O}$ [26] that we had reported previously. The central $\text{Nd}(\text{III})$ is coordinated to two amine nitrogens and seven oxygens of which one ($\text{O}(11)$) belongs to coordinated water. The remaining two amine nitrogens, four carboxyl oxygens, and two ethyleneglycol oxygens all come from one octadentate Egta $^{4-}$. The reason that the $\text{Nd}(\text{III})$ adopts a nine-coordinate conformation due to its larger ionic radius, which generates a relatively small coordination number. Meanwhile, it has a mononuclear molecular structure. The center metal Nd^{3+} ion in **I** is surrounded by two amine N atoms ($\text{N}(1)$ and $\text{N}(2)$) and six carboxylic O atoms ($\text{O}(1)$,

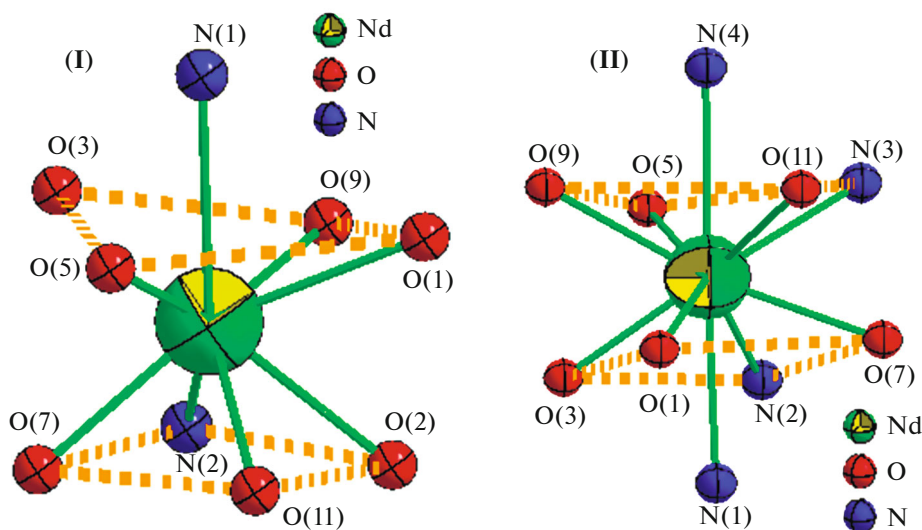


Fig. 2. Coordination polyhedron around Nd(III) in I and II.

O(2), O(3), O(5), O(7) and O(9)), all come from one Egta⁴⁻ ligand. The two N atoms and six O atoms of one Egta⁴⁻ ligand create seven five-membered chelating rings with the central Nd³⁺ ion, in which the four atoms are almost coplanar in each ring.

Obviously, the Nd³⁺ ion in this [Nd^{III}(Egta)H₂O]⁻ complex anion is mononuclear nine-coordinate geometry with pseudo-monocapped square antiprismatic (MC-SAP) conformation which is similar with (EnH₂)[Er^{III}(Egta)(H₂O)]₂ · 6H₂O, and (EnH₂)[Ho^{III}(Egta)(H₂O)]₂ · 6H₂O (seen from Fig. 2a). In the coordinate atoms around Nd(III), the set of O(1), O(3), O(5), and O(9) and the set of O(2), O(7), O(11), and N(2) make two approximate parallel square planes. The capped position is occupied by N(1) above the plane of O(1), O(3), O(5), and O(9). The repulsion between the capped atom N(1), and the top plane formed by O(1), O(3), O(5), and O(9) make the Nd–N(1) bond distance (2.679(3) Å) shorter than Nd–N(2) (2.695(3) Å) bond distance. The set of O(1), O(3), O(5), and O(9) and the set of O(2), O(7), O(11), and N(2) form two approximate square (top and bottom) planes, respectively, which are basically parallel to each other and the torsion angle is about 45°. Furthermore, the upper quadrilateral plane is formed by one ethyleneglycol (O(1)) atom, three carboxyl O atoms (O(3), O(5), and O(9)), the bottom quadrilateral plane is formed by one ethyleneglycol (O(2)) atom, coordination water O atom (O(11)), one carboxyl O atoms (O(7)) and one amine N atoms (N(2)).

In addition, from Fig. 2a, it can be calculated that the value of the square antiprism angle, to the upper quadrilateral plane, the average value of the trigonal dihedral angle between $\Delta(O(3)O(5)O(9))$ and $\Delta(O(5)O(9)O(1))$ is $\sim 14.29^\circ$, and between

$\Delta(O(5)O(3)O(1))$ and $\Delta(O(3)O(1)O(9))$ is $\sim 14.98^\circ$. To the bottom plane, the value of the dihedral angle between $\Delta(O(2)N(2)O(11))$ and $\Delta(N(2)O(11)O(7))$ triangles is 5.75° , and between $\Delta(N(2)O(2)O(7))$ and $\Delta(O(2)O(7)O(11))$ triangle it is 5.06° . According to these calculated data and Guggenberger and Muetterties' method [27], these data are much less than than 26.4° , we can firmly draw a conclusion that the conformation of Nd(1)N₂O₇ in the [Nd^{III}(Egta)H₂O]⁻ complex anion indeed keeps a pseudo-MC-SAP conformation.

As shown in Table 2, for I, the Nd(1)–O bond distances vary from 2.407(3) Å (Nd(1)–O(7)) to 2.576(3) Å (Nd(1)–O(1)). Furthermore, the bonds distance of Nd(1)–O(1) and Nd(1)–O(2) (both belonging to ethyleneglycol O atoms) are somewhat longer than the bonds distances of Nd(1)–O(3), Nd(1)–O(5), Nd(1)–O(7), and Nd(1)–O(9) (both belonging to carboxylic O atoms), which indicates that the O atoms which come from coordinate carboxylic more stably than ethyleneglycol O atoms (O(1) and O(2)). This is consistent with the findings with Egta⁴⁻ ligands made by previously reported. While the Nd(1)–N bond distances range from 2.695(3) Å (Nd(1)–N(2)) to 2.679(3) Å (Nd(1)–N(1)). From the above, its apparently that Nd(1)–O bonds are much stable than Nd(1)–N bonds. Table 2 also shows a series of bond angles, for instance, the ONd(1)O bond angles in I is range from 65.57(9)° (O(2)Nd(1)O(11)) to 157.12(10)° (O(1)Nd(1)O(7)), ONd(1)N bond angles vary from 62.91(10)° (O(3)Nd(1)N(1)) to 148.04(11)° (O(5)Nd(1)N(2)), and the N(1)Nd(1)N(2) bond angles is 128.03(10)°. Among them, the largest angle is 157.12(10)° (O(1)Nd(1)O(7)) and the smallest bond angle is 62.91(10)° (O(3)Nd(1)N(1)). Although there are

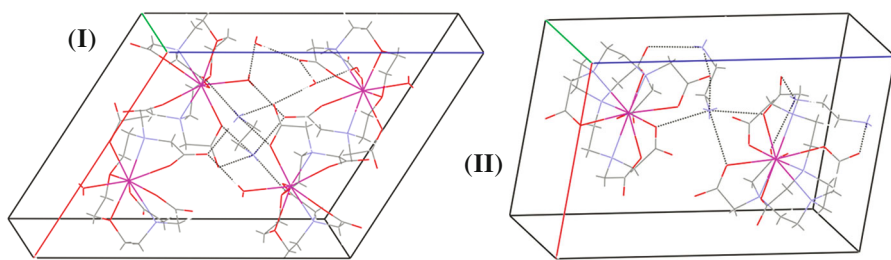


Fig. 3. Arrangements of I and II in unit cell (dashed lines represent intermolecular hydrogen bonds).

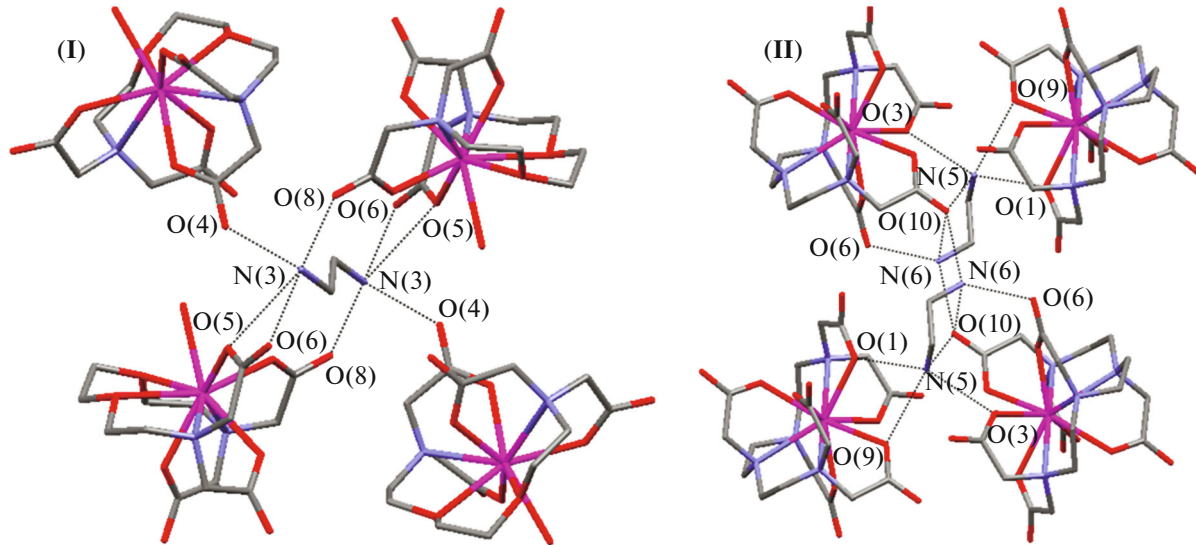


Fig. 4. Bindings between EnH_2^{2+} and $[\text{Nd}^{\text{III}}(\text{Egta})\text{H}_2\text{O}]^-$ in I and $[\text{Nd}^{\text{III}}(\text{Ttha})]^{3-}$ in II (dashed lines represent intermolecular hydrogen bonds).

some distorted, the conformation around Nd(1) indeed keeps a square antiprism conformation.

As shown in Fig. 3a, there are four molecules of I in a unit cell. The complex molecules connect with each other through hydrogen bonding and EnH_2^{2+} . Therefore, as a whole crystal, a network structure is formed through hydrogen bonds and electrostatic bonding. In addition, the hydrogen bonds play an important role in the structure of I. As seen from Fig. 4a, the EnH_2^{2+} cation is located in a center symmetric structure. Obviously, each EnH_2^{2+} cation with four adjacent $[\text{Nd}^{\text{III}}(\text{Egta})\text{H}_2\text{O}]^-$ complex anions forms hydrogen bonds. That is, N(3) connects four O atoms (O(4), O(5), O(6) and O(8)), in which O(5), O(6) come from the same carboxyl group of $[\text{Nd}^{\text{III}}(\text{Egta})\text{H}_2\text{O}]^-$ complex anion, and the O(4) and O(8) come from two carboxyl groups of two $[\text{Nd}^{\text{III}}(\text{Egta})\text{H}_2\text{O}]^-$ complex anions, respectively. The distances of N(3)…O(4), N(3)…O(5), N(3)…O(6), and N(3)…O(8) are 2.756, 3.040, 2.806, and 2.782 Å, respectively.

As shown in Fig. 5a, every four $[\text{Nd}^{\text{III}}(\text{Egta})\text{H}_2\text{O}]^-$ complex ions are interconnected together by sharing ethylenediamine (N(3)–C(15)–C(15)–N(3)), forming a basic SBU. The two neighboring SBU are further connected resulting in the formation of 2D network in plane. Owing to this special coordination environment, the Newman' pattern dihedral angle of ethylenediamine is exactly 180°. Thus, four atoms of ethylenediamine all locate in the same plane. Therefore, it can be observed that amino acids as a part of protein can interact with $[\text{Nd}^{\text{III}}(\text{Egta})\text{H}_2\text{O}]^-$ complex anion through different binding manner.

As shown in Fig. 1b, it shows that the nine-coordinated structure of II is a 1 : 1 proportion of rare earth metal ions to ligand stoichiometry, its molecular and crystal structures is different in respect to I mentioned above. Figure 1b has also shown the molecular structure of II complex. The central Nd^{3+} ion is ten-coordinated with one H_6Ttha ligand by four nitrogen atoms and six carboxylic oxygen atoms, which come from the same H_6Ttha ligand. Unlike the complex of I, without

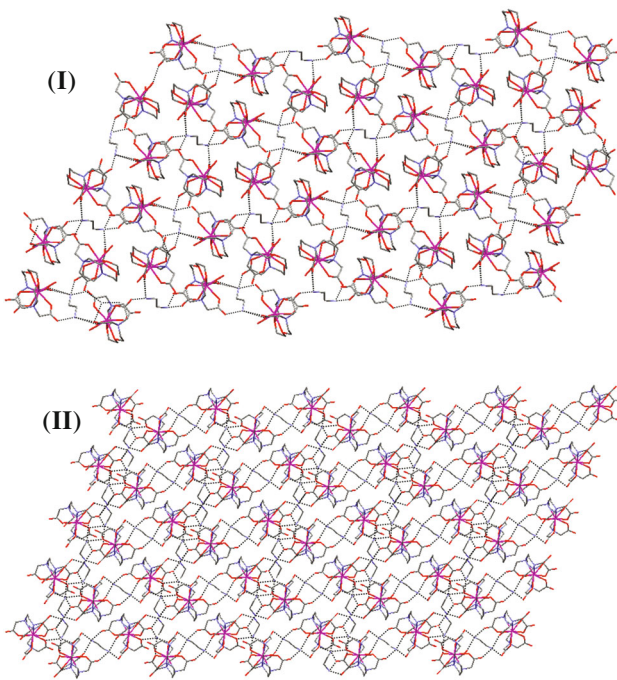


Fig. 5. Polyhedral view of the 2D ladder-like layered network of I and II.

a coordination water molecule, the ten atoms from one H_6Ttha ligand shape seven structurally stable five-member rings with Nd^{3+} ion as well as the atoms in each five-member ring are almost coplanar.

Evidently, the coordination geometry around the central Nd^{3+} ion in $[\text{Nd}^{\text{III}}(\text{Ttha})]^{3-}$ complex anion is a ten-coordinate distorted bicapped square antiprismaticprism (Fig. 2b). Furthermore, the capping donor atom N(4) locates the above quadrilateral plane. The above quadrilateral plane of antiprism is formed by three carboxyl O atoms (O(3), O(5) and O(9)) and one amine N atom (N(3)). While the bottom quadrilateral plane is done by one amine N atom (N(2)), three carboxyl O atom (O(1) O(3) and O(7)). In addition, as seen from Fig. 2b, it also can be found that the $\text{Nd}(\text{III})\text{N}_2\text{O}_6$ part is not standard bicapped square antiprism. To the upper plane, the average value of the bicapped square antiprism angle between $\Delta(\text{O}(5)\text{O}(9)\text{N}(3))$ and $\Delta(\text{O}(9)\text{N}(3)\text{O}(11))$ is about 10.55° , and between $\Delta(\text{O}(9)\text{O}(5)\text{O}(11))$ and $\Delta(\text{O}(5)\text{O}(11)\text{N}(3))$ is about 10.29° . The nether plane, the average value of the bicapped square antiprism angle between $\Delta(\text{O}(1)\text{O}(3)\text{O}(7))$ and $\Delta(\text{O}(3)\text{O}(7)\text{N}(2))$ is $\sim 4.02^\circ$, and between $\Delta(\text{O}(3)\text{O}(1)\text{N}(2))$ and $\Delta(\text{O}(1)\text{N}(2)\text{O}(7))$ is $\sim 4.20^\circ$. According to these calculated data and Guggenberger and Muetterties' method, we may safely come to conclusion that the conformation of $\text{Nd}(\text{III})\text{N}_2\text{O}_6$ in $[\text{Nd}^{\text{III}}(\text{Ttha})]^{3-}$ complex anion indeed keeps a bicapped square antiprism polyhedron but distorted to a small extent.

The series of bond distances for **II** are given in Table 2. The lengths of all $\text{Nd}(1)-\text{O}$ bonds are in the wide varying from $2.455(4)$ Å ($\text{Nd}(1)-\text{O}(5)$) to $2.586(6)$ Å ($\text{Nd}(1)-\text{O}(11)$) with an average value of $2.496(5)$ Å. By comparison it can be found that, bond distances for **II** is somewhat longer than the corresponding value ($2.407(3)$ to $2.576(3)$ Å) in **I**, indicating that the complex of **I** is more stable than **II**. While the two $\text{Nd}(1)-\text{N}$ bond distances are $2.719(6)$ Å ($\text{Nd}(1)-\text{N}(3)$) and $2.789(7)$ Å ($\text{Nd}(1)-\text{N}(4)$) with an average value of $2.749(6)$ Å. So, we firmly conclude that the O atoms coordinate to the central Nd^{3+} ion much stronger than the N atoms, since $\text{Nd}(\text{III})-\text{N}$ bond lengths are significantly longer than the $\text{Nd}(\text{III})-\text{O}$ bond lengths. In addition, Table 2 illustrates a series of bond angles. The OndO bond angles are placed changing from $64.58(17)^\circ$ ($\text{O}(7)\text{Nd}(1)\text{O}(11)$) to $157.12(17)^\circ$ ($\text{O}(7)\text{Nd}(1)\text{O}(9)$). The OndN bond angles vary from $60.06(19)^\circ$ ($\text{O}(9)\text{Y}(1)\text{N}(4)$) to $142.97(18)^\circ$ ($\text{O}(1)\text{Y}(1)\text{N}(3)$). Meanwhile, the NNdN bond angles are placed changing from $65.94(19)^\circ$ ($\text{N}(3)\text{Nd}(1)\text{N}(4)$) to $125.16(17)^\circ$ ($\text{N}(2)\text{Nd}(1)\text{N}(4)$). Among them, the smallest and largest bond angles are $60.06(19)^\circ$ ($\text{O}(9)\text{Y}(1)\text{N}(4)$) and $157.12(17)^\circ$ ($\text{O}(7)\text{Nd}(1)\text{O}(9)$), respectively. Thus, all these obviously distort the geometrical configuration of $\text{Nd}(\text{III})\text{N}_2\text{O}_6$ part in $[\text{Nd}^{\text{III}}(\text{Ttha})]^{3-}$.

In one unit cell, as seen in Fig. 3b, there are two molecules of **II**. The molecules connect with each other through hydrogen bonds and electrostatic forces with crystallization water and EnH_2^{2+} , which contribute to stabilizing the crystal structure. In addition, the hydrogen bonds play an important role in the construction of 2D ladder-like network structure of **II**. As seen from Fig. 4b, the two cations (EnH_2^{2+}) is located in a center symmetric structure, and the symmetric center is in the middle position of the two EnH_2^{2+} cations. Obviously, the EnH_2^{2+} cation with three adjacent $[\text{Nd}^{\text{III}}(\text{Ttha})]^{3-}$ complex anions forms hydrogen bonds. That is, each N(5) connect with four carboxyl O atoms (O(1), O(3), O(9) and O(10)), in which O(1) and O(9) come from two carboxyl groups of one $[\text{Nd}^{\text{III}}(\text{Ttha})]^{3-}$ complex anion, and O(3) and O(10) come from adjacent two carboxyl groups of one $[\text{Nd}^{\text{III}}(\text{Ttha})]^{3-}$ complex anion. The hydrogen bond distances of $\text{N}(5)\cdots\text{O}(1)$, $\text{N}(5)\cdots\text{O}(3)$, $\text{N}(5)\cdots\text{O}(9)$, $\text{N}(5)\cdots\text{O}(10)$, $\text{N}(6)\cdots\text{O}(6)$, $\text{N}(6)\cdots\text{O}(10B)$ and $\text{N}(6)\cdots\text{O}(10C)$ are 2.764 , 2.785 , 3.138 , 3.017 , 2.788 , 2.724 , and 2.955 Å, respectively (Table 3). Shown in Fig. 5b, every four $[\text{Nd}^{\text{III}}(\text{Ttha})]^{3-}$ complex anions are interconnected together by sharing ethylenediamine ($\text{N}(5)-\text{C}(19)-\text{C}(20)-\text{N}(6)$), forming a basic SBU (secondary building units). The two neighboring SBU are further linked leading to the formation of 2D network in plane.

Table 3. Geometric parameters of hydrogen bonds of **I** and **II**

D—H…A	Distance, Å			Angle DHA, deg	Symmetry code
	D—H	H…A	D…A		
I					
N(3)—H(3A)…O(4)	0.89	1.87	2.756(10)	177	$-x + 1, y - 1/2, -z + 3/2$
N(3)—H(3B)…O(6)	0.89	1.92	2.806(11)	171	$-x + 1, -y + 1, -z + 2$
N(3)—H(3B)…O(5)	0.89	2.56	3.040(11)	115	$-x + 1, -y + 1, -z + 2$
N(3)—H(3C)…O(8)	0.89	1.92	2.782(9)	162	$x, y - 1, z$
N(3)—H(3C)…O(7)	0.89	2.63	3.359(9)	139	$x, y - 1, z$
II					
N(5)—H(5A)…O(1)	0.89	1.96	2.764(17)	149	
N(5)—H(5B)…O(9)	0.89	2.38	3.035(17)	131	
N(5)—H(5B)…O(4)	0.89	2.48	3.107(18)	128	$-x + 1, -y + 1, -z + 1$
N(5)—H(5C)…O(3)	0.89	2.24	2.785(16)	119	$-x + 1, -y + 1, -z + 1$
N(5)—H(5C)…O(9)	0.89	2.32	3.138(16)	153	$-x + 1, -y + 1, -z + 1$
N(5)—H(5C)…O(10)	0.89	2.55	3.017(17)	114	$-x + 1, -y + 1, -z + 1$
N(6)—H(6A)…O(6)	0.89	1.90	2.788(17)	171	$-x + 1, -y + 1, -z + 1$
N(6)—H(5B)…O(10)	0.89	1.86	2.724(18)	162	$x - 1, y, z$
N(6)—H(5C)…O(10)	0.89	2.08	2.955(16)	166	$-x + 1, -y + 1, -z + 1$
N(7)—H(7A)…O(8)	0.89	1.90	2.771(17)	167	$-x + 1, -y + 2, -z + 2$
N(7)—H(7B)…O(2)	0.89	1.98	2.791(18)	150	
N(7)—H(7C)…O(12)	0.89	1.89	2.769(16)	169	
N(7)—H(7C)…O(11)	0.89	2.63	3.129(18)	116	

ACKNOWLEDGMENTS

The authors greatly acknowledge the National Science Foundation of China (21371084), Shenyang Science and Technology Plan Project (F13-289-1-00), Key Laboratory Basic Research Foundation of Liaoning Provincial Education Department (L2015043) and Liaoning Provincial Department of Education Innovation Team Projects (LT2015012) for financial support. The authors also thank our colleagues and other students for their participating in this work.

REFERENCES

1. Bünzli, J.C.G. and Piguet, C., *Chem. Rev.*, 2002, vol. 102, p. 1897.
2. Tsukube, H. and Shinoda, S., *Chem. Rev.*, 2002, vol. 102, p. 2389.
3. Laurent, S., Vander Elst, L., Wautier, M., et al., *Bioorg. Med. Chem. Lett.*, 2007, vol. 17, p. 6230.
4. Sink, R.M., Buster, D.C., and Sherry, A.D., *Inorg. Chem.*, 1990, vol. 29, p. 3654.
5. Pei, J., Geng, X.T., Yan, J.B., et al., *J. Alloys Compd.*, 2006, vol. 426, p. 363.
6. Moynagh, J. and Schimmel, H., *Nature*, 1999, vol. 400, p. 105.
7. Kang, J.G., Hong, J.P., and Yoon, S.K., *J. Alloys Compd.*, 2002, vol. 339, p. 248.
8. Ozolins, M. and Eichler, H.J., *Appl. Phys. Lett.*, 2000, vol. 77, p. 615.
9. Yuan, J.L. and Wang, G.L., *TrAC-Trends. Anal. Chem.*, 2006, vol. 25, p. 490.
10. Ohashi, H., Hachiya, K., Yoshida, et al., *J. Alloys Compd.*, 2004, vol. 373, p. 1.
11. Fan, W., Chen, L.X., Liu, X.W., et al., *Chinese-German J. Clin. Oncol.*, 2007, vol. 6, p. 396.
12. Neves, M., Gano, L., Pereira, N., et al., *Nucl. Med. Biol.*, 2002, vol. 29, p. 329.
13. Beeby, A., Botchway, S.W., Clarkson, I.M., et al., *J. Photochem. Photobiol. B*, 2000, vol. 57, p. 83.

14. Terai, T., Kikuchi, K., Iwasawa, S., et al., *J. Am. Chem. Soc.*, 2006, vol. 128, p. 6928.
15. Accardo, A., Tesauro, D., and Aloj, L., *Coord. Chem. Rev.*, 2009, vol. 253, p. 179.
16. Efthimiaou, E.K., Katsarou, M.E., and Fardis, M., *Bioorg. Med. Chem. Lett.*, 2008, vol. 18, p. 6058.
17. Khreis, O.M., Curry, R.J., Somerton, M., and Gillin, W.P., *J. Appl. Phys.*, 2000, vol. 88, p. 777.
18. Li, Z.F., Yu, J.B., Zhou, L., et al., *Inorg. Chem. Commun.*, 2009, vol. 12, p. 151.
19. Gao, J.Q., Li, D., Wang, J., et al., *J. Coord. Chem.*, 2011, vol. 64, p. 2231.
20. Xua, R., Lia, D., Wang, J., et al., *Russ. J. Coord. Chem.*, 2010, vol. 36, p. 810.
21. Wang, J., Hua, P., Liu, B., et al., *Russ. J. Coord. Chem.*, 2010, vol. 36, p. 232.
22. Wang, J., Li, D., Gao, J.Q., et al., *J. Coord. Chem.*, 2010, vol. 63, p. 3792.
23. Bai, Y., Gao, J.Q., Wang, J., et al., *J. Coord. Chem.*, 2013, vol. 66, p. 367.
24. Bai, Y., Gao, J.Q., Wang, J., et al., *J. Coord. Chem.*, 2013, vol. 39, p. 147.
25. Gao, J.Q., Wu, T., Wang, J., et al., *J. Coord. Chem.*, 2011, vol. 37, p. 817.
26. Gao, J.Q., Li, D., Wang, J., et al., *J. Coord. Chem.*, 2013, vol. 64, p. 2234.
27. Guggenberger, L.J. and Muetterties, E.L., *J. Am. Chem. Soc.*, 1976, vol. 98, p. 7221.